

Light-induced multistep redox reactions: The diode-array spectrophotometer as a photoreactor*

István Fábíán[‡] and Gábor Lente

*Department of Inorganic and Analytical Chemistry, University of Debrecen,
P.O.B. 21, H-4010, Debrecen, Hungary*

Abstract: The light source of a photometer may induce chemical reactions in photosensitive reactive systems. Diode-array spectrophotometers are particularly suitable for producing such phenomena. This paper provides an overview on how this equipment can be used as a photoreactor. The principles of various techniques to control the intensity and spectral region of the illuminating light are discussed in detail. It will be shown that the quantum yields of various photochemically induced redox reactions can be determined by exploiting specific features of diode-array spectrophotometers. Kinetic coupling between primary photochemical and secondary thermally activated reaction steps are utilized to explore intimate details of composite redox reactions. Key aspects of the method applied are demonstrated via the photoreactions of 2,6-dichloro-1,4-benzoquinone (DCQ), the photoinduced autoxidation of S(IV) and a photochemically activated redox reaction of the chlorate ion.

Keywords: autoxidation; chlorate ion; diode-array spectrophotometer; photoinitiation; quantum yield; spectrophotometry; sulfur(IV).

INTRODUCTION

Spectrophotometry is a standard tool of the chemical trade. The basic principles of this experimental technique are well established and discussed in chemical textbooks in detail [1–3]. Spectrophotometers are standard equipment in any chemical laboratory, and they are extensively used for a variety of purposes, such as quantitative determination of various compounds, characterizing spectral features of a wide range of chemical species, monitoring the kinetics of chemical processes, etc. In general, spectrophotometers are considered to be very routine instruments with no particularly exciting features. However, sometimes spectrophotometers may produce unexpected phenomena in photosensitive systems because the absorption of light by one or more species may trigger photochemically induced processes. When such events are not recognized, the interpretation of the experimental data may be completely skewed. For example, the kinetics of the reaction between chlorate ion and iodine was first reported as a thermally activated process [4], but later it was pointed out that the spectrophotometric experimental method itself provided initiating light and the actual reaction is exclusively photochemical [5]. A very similar sequence of events occurred earlier in the investigation of the chemical reaction between chlorine dioxide and chloride ion [6]. On the other hand, the exact features that may lead to embarrassing mistakes also offer novel possibilities for studying the kinetics of a series of reactions, in-

*Paper based on a presentation at the 31st International Conference on Solution Chemistry (ICSC-31), 21–25 August 2009, Innsbruck, Austria. Other presentations are published in this issue, pp. 1855–1973.

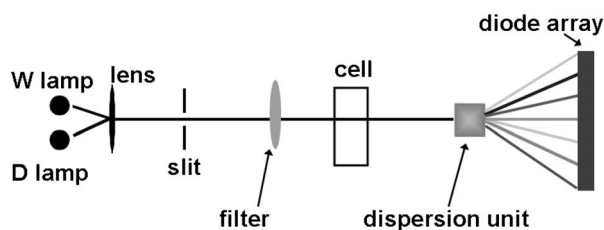
[‡]Corresponding author: E-mail: ifabian@delfin.unideb.hu

cluding photoactive species as reactants. In this study, we discuss the basic principles of using a spectrophotometer as a photoreactor and demonstrate how such a device can be used to explore mechanistic aspects of complicated kinetic reactions. Although the basic concept discussed here can be used both in gaseous and liquid phase, experimental limitations and the general design of commercially available spectrophotometers make these studies feasible in liquid phase. The results covered in this paper were obtained in aqueous solutions [5,7–10].

GENERAL CONSIDERATIONS

In any spectrophotometer, a light beam is projected to the sample and the amount of light transmitted is measured as a function of wavelength. The light is typically dispersed before the beam hits the sample in a regular single- or double-beam spectrophotometer. It follows that only a relatively low-intensity, narrow-bandwidth “monochromatic” light passes through the sample at any moment when a spectrum is recorded. Exposure to light at any wavelength depends on the scanning rate of the equipment and the bandwidth. In most instruments, the monochromator rests at high wavelengths between scans and photochemical reactions are not expected to occur under these conditions, although such a possibility cannot be completely excluded.

The design of diode-array spectrophotometers is quite different from that of their common sisters. The general design of such spectrophotometers is shown in Scheme 1. The light source of the instrument consists of a deuterium and a halogen lamp. Because of the relatively low sensitivity of the detector, the intensities of the lamps are high. The polychromatic light is not dispersed until it passes the sample, i.e., the monochromator is placed after the cell holder. Thus, an undispersed and relatively high-intensity light passes through the sample during the whole measurement. In most of the instruments, the spectrum covers the 190–1100 nm spectral range. Direct measurement of light intensity reveals that the highest photon counts occur at shorter wavelengths, i.e., the flux of high-energy photons is relatively high. Thus, photochemical reactions can easily be triggered in these instruments provided that the sample contains reactive species sensitive to light. This feature may complicate certain spectrophotometric measurements, but it also offers an excellent possibility to use spectrophotometers for studying photo-initiated reactions. Optical filters (cf. Scheme 1) make it possible to control the light intensity as well as the spectral range of the illuminating light. In order to take full advantage of using diode-array spectrophotometers as photoreactors, the number of photons passing through the sample needs to be determined either by direct measurements or by using appropriate calibration methods.



Scheme 1 General design of a diode-array spectrophotometer.

When a spectrophotometer is used for photochemical studies, excitation of the photoactive species and monitoring the progress of photochemically induced reactions occur simultaneously. It should be emphasized that such an experimental design does not make it possible to follow primary photochemical events such as the formation of excited species, excitation transfer, etc. because the lifetimes of these reactions are orders of magnitude shorter than the time resolutions of commercially available diode-array spectrophotometers. However, the progress of the photochemically induced reactions

can easily be monitored. Primary photochemical reactions are restricted to a certain location in the cell where the light is actually absorbed by the sample, i.e., the whole amount of the sample is not illuminated and even the light intensity may vary along the cross-section of the light beam. This results in inhomogeneity in the spatial distribution of the photochemical events, which eventually results in irreproducible kinetics traces. Figure 1 gives an example of this phenomenon [7]. Constant stirring of the reaction mixtures during the kinetic measurements circumvents this problem. The definite need for stirring to obtain reproducible results may indicate photochemical interference during spectrophotometric measurements.

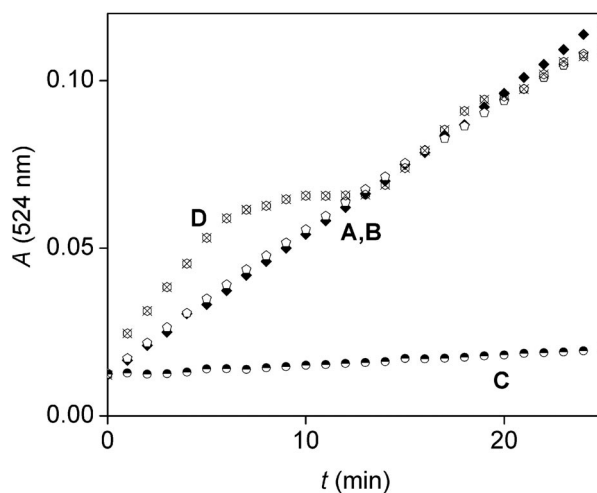


Fig. 1 Kinetic traces measured in the aqueous photoreaction of DCQ. [DCQ] = 1.08 mM, and path length = 1 cm for all curves. $T = 25.0\text{ }^{\circ}\text{C}$ (trace A, C, and D); $T = 10.0\text{ }^{\circ}\text{C}$ (trace B); no stirring for trace D; only the visible lamp was used for trace C.

When a photosensitive reactive system is illuminated, essentially a new reactant, the photon, is introduced in a well-controlled fashion. Because of the constant flux of photons, the rate of the photo-initiation step is constant when the photoactive species is used in sufficient excess and its concentration change is negligible during the measurement. These features are very useful when the applicable concentration ranges of the other reactants are limited for practical reasons.

Reactive intermediates play an important kinetic role in complex redox systems. In thermally activated reactions, the steady-state concentrations of these species are determined by the rates of their formation and subsequent reactions with each other and the reactants. Typically, the variation of the reactant concentrations affects all of these rates in a very complex manner, and the separation of the contributions of the individual reaction steps to the overall process is a painstaking task. Strong kinetic coupling between the competing reaction paths quite often makes only provisional interpretation of mechanistic aspects of the overall reaction possible. In certain systems, photoinitiation can be used to control the rate of the formation of the reactive intermediates independently from the rates of subsequent reaction steps. This may provide an easier way to understand the kinetic significance of each of the co-existing reaction steps. In other words, photoinitiation may lead to kinetic coupling between photochemically and thermally activated reaction steps and be used as an efficient tool to explore the mechanisms of complex redox reactions.

COUNTING PHOTONS

A quantitative evaluation of photochemical experiments carried out by diode-array spectrophotometers cannot be done in the standard photochemical way. There are two main problems: the light used to drive the reaction is polychromatic, and the instrument is not originally designed for such measurements. However, some resourcefulness can go a long way in solving these problems. First of all, the photon flow (Φ_P) going through the absorption cuvette must be determined (photochemical terms used here strictly adhere to IUPAC recommendations wherever they exist [11]). This is most conveniently done through the spectral photon flow, $\Phi_{P\lambda}$, to accommodate the polychromatic nature of light. Optical properties related to $\Phi_{P\lambda}$ are often measured by spectrophotometers.

$$\Phi_P = \int_{\lambda_{\min}}^{\lambda_{\max}} \Phi_{P\lambda} d\lambda \quad (1)$$

Thus far, our group has experience with two different diode-array spectrophotometers, an HP-8543 and a Shimadzu MultiSpec-1500, which are both single-beam instruments. In the HP instrument, a quantity directly proportional (but not identical) to the spectral photon flow can be measured in the diagnostic mode of the instrument, which is called number of counts at a given wavelength (N_λ)

$$\Phi_{P\lambda} = C_1 N_\lambda \quad (2)$$

where C_1 is a scaling constant specific to the instrument but independent of wavelength or measurement time. The Shimadzu instrument is calibrated to measure spectral irradiance (E_λ) directly. However, the beam geometry cannot be measured with any reasonable accuracy and in practice, a scaling constant (C_2^*) is also needed here. In addition, the calculation also involves some natural constants (h : Planck's constant, c : speed of light, N_A : Avogadro's constant)

$$\Phi_{P\lambda} = \frac{C_2^* E_\lambda h c}{\lambda N_A} = \frac{C_2 E_\lambda}{\lambda} \quad (3)$$

In the given final formula, C_2^* is combined with the natural constants to yield a single constant C_2

$$C_2 = C_2^* h c / N_A \quad (4)$$

The part of the photon flow that is absorbed in a solution, N , was termed absorbed photon count for the lack of an IUPAC-approved name in one of our earlier works [7]. This can be calculated from the spectral photon flow using the absorbance measured in the spectrophotometer

$$N = \int_{\lambda_{\min}}^{\lambda_{\max}} \Phi_{P\lambda} (1 - 10^{-A_\lambda}) d\lambda \quad (5)$$

The entire spectral range of the instrument should be included in the integration. However, the nature of this equation is such that ignoring the region where the solution does not absorb ($A = 0$) obviously does not change the result. In addition, the physical wavelength resolution (i.e., the number of diodes in the array) of the spectrophotometers is usually not better than ca. 1 nm, although in the case of the Shimadzu instrument, electronic resolution enhancement makes it possible to have absorbance readings every 0.1 nm. Therefore, summation from the minimum to the maximum wavelength with an interval of 1 nm can replace the integration in actual calculations using eq. 5. If the photoactive component is the only absorbing species, the rate of primary photochemical (v_{primary}) processes can be calculated as

$$v_{\text{primary}} = \sum_{\lambda_{\text{min}}}^{\lambda_{\text{max}}} \Phi_{\lambda} C_1 N_{\lambda} (1 - 10^{-A_{\lambda}}) \quad (6)$$

or

$$v_{\text{primary}} = \sum_{\lambda_{\text{min}}}^{\lambda_{\text{max}}} \Phi_{\lambda} \frac{C_2 E_{\lambda}}{\lambda} (1 - 10^{-A_{\lambda}}) \quad (7)$$

In these formulas, Φ_{λ} is the differential quantum yield at wavelength λ [11]. If there are other absorbing species in the system, the fraction of light actually absorbed by the active species should be calculated. Assuming n absorbing species with concentrations c_i and molar absorption coefficients ε_i each (c_{act} and ε_{act} being corresponding parameters for the photoactive species) gives additional terms in eqs. 6 and 7.

$$v_{\text{primary}} = \sum_{\lambda_{\text{min}}}^{\lambda_{\text{max}}} \frac{\varepsilon_{\text{act}} c_{\text{act}}}{\sum_{i=1}^n \varepsilon_i c_i} \Phi_{\lambda} C_1 N_{\lambda} (1 - 10^{-A_{\lambda}}) \quad (8)$$

or

$$v_{\text{primary}} = \sum_{\lambda_{\text{min}}}^{\lambda_{\text{max}}} \frac{\varepsilon_{\text{act}} c_{\text{act}}}{\sum_{i=1}^n \varepsilon_i c_i} \Phi_{\lambda} \frac{C_2 E_{\lambda}}{\lambda} (1 - 10^{-A_{\lambda}}) \quad (9)$$

Equations 6–9 can be used in two ways for photochemical studies. For a photochemical reaction with known quantum yield, constants C_1 or C_2 can be calculated after measuring the rate of the reaction. The most suitable method for this has been ferrioxalate actinometry thus far [12,13]. There is a lot of information on the spectral variation of the quantum yield in this system [13], and interpolation can be used readily to generate quantum yields with the required 1-nm resolution. Another use of these equations is for previously unknown photochemical processes: after actinometric determination of the values of C_1 or C_2 , quantum yields can be calculated from measured reaction rates. Very formally, any of these values will be a weighted average over the spectral range used and different weighted averages will be available by using spectral filters. However, this is rarely a major problem as quantum yields typically do not depend on wavelength much. A single measurement gives an estimate for the quantum yield, but it is better to carry out several different measurements. Plotting the rate of a simple photochemical process as a function of photon count yields a straight line (Fig. 2), the slope of which can be used to calculate Φ [7]. The figure also contains some points in which NaNO_3 was added to the studied solution so that the inner filter effect of this otherwise innocent salt changed the photon count.

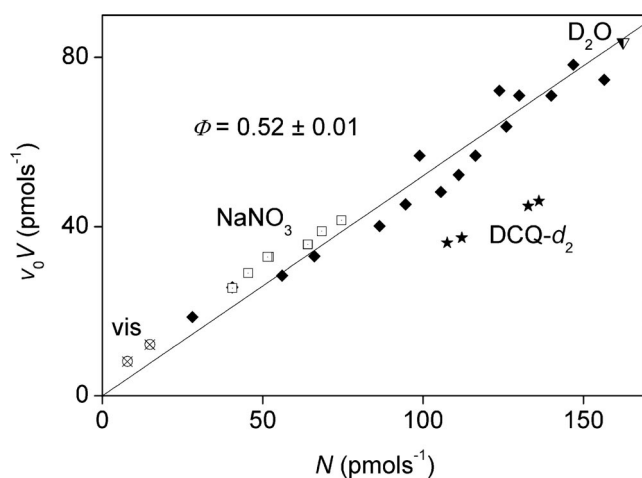


Fig. 2 Reaction rate in the aqueous photoreaction of DCQ as a function of photon counts. $T = 25.0$ °C. vis (circles): using the visible lamp only as a driving force. D₂O (triangle): experiment done in D₂O. NaNO₃ (squares): experiments done in the presence of NaNO₃. DCQ-*d*₂ (stars): experiments done using DCQ-*d*₂ dissolved in H₂O.

CONTROLLING THE INTENSITY OF LIGHT

Spectrophotometers have fixed and carefully stabilized light sources. Therefore, changing the intensity of the driving light seems to be difficult at first sight. However, some creative thinking can also provide useful solutions here.

The first method is to change the volume of the investigated sample because this does not affect the overall photon flow from the light source as can be easily understood if one thinks in terms of photon flow per unit volume. Changing the volume in a photometric cell does not change any of the chemical concentrations, but does change the amount of light absorbed in a unit volume, i.e., the absorbed photon “concentration” if the sample is constantly stirred. The larger the volume is, the smaller amount of light is absorbed in a unit volume. Unfortunately, the volume change is severely limited by the geometrical constraint that the entire light beam must still go through the solution, i.e., it must pass the sample below the meniscus. In the HP instrument, this factor allows the volume to be changed from 1.7 to 3.4 cm³ in a standard photometric cell (path length: 10 mm), therefore, the light intensity can be varied by a factor of two. This is not a very wide range, but is suitable for drawing basic conclusions as demonstrated in Fig. 3. The plots of the logarithm of the reaction rate as a function of the logarithm of sample volume confirm that the reaction is first-order and 0.5-order with respect to the absorbed photon count in the uncatalyzed [8] and the Ce(III)-catalyzed [9] autoxidation of S(IV), respectively.

Larger changes in intensity can be reached by physical light blocking, for example, by inserting perforated metal sheets (e.g., simply an aluminum foil) into the light beam in the place indicated for filters in Scheme 1. The amount of light blocked can simply be measured by the spectrophotometer by taking the baseline without the blocking device and then recording a spectrum (preferably in transmittance mode) in the presence of the blocker. In our practice, this method allowed a variation of intensity by a factor of 20, the lower limit of light intensity being only determined by the convenience of following rather slow photochemical reactions.

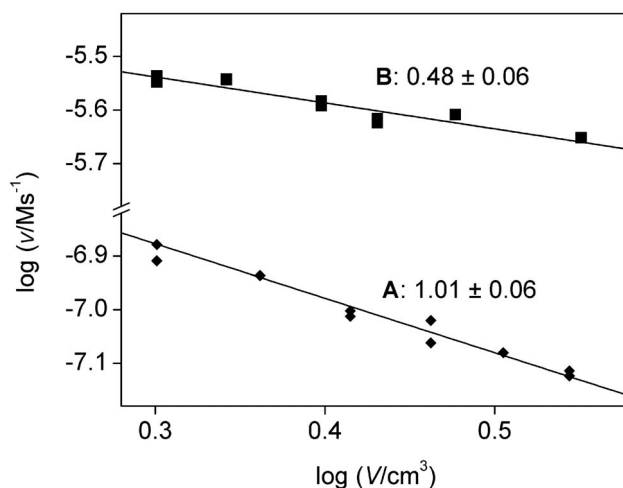


Fig. 3 Dependence of reaction rates on sample volume in the uncatalyzed (A) and Ce(III)-catalyzed (B), photoinitiated autoxidation of S(IV). The order of the reaction rate with respect to the absorbed photon count is given in the figure. $T = 25.0\text{ }^{\circ}\text{C}$, $[\text{O}_2] = 0.23\text{ mM}$ and path length: 1.000 cm for both systems. (A) $[\text{S(IV)}] = 2.00\text{ mM}$, $[\text{H}_2\text{SO}_4] = 0.50\text{ M}$ (B) $[\text{Ce}^{3+}] = 0.50\text{ mM}$; $[\text{S(IV)}] = 1.00\text{ mM}$; $[\text{H}_2\text{SO}_4] = 0.10\text{ M}$.

Various filters can also be used in place of the blocking device described in the previous paragraph. These can be actual filters manufactured for photochemical purposes, but any other object will do which absorbs some light in the useful wavelength region. Quartz cuvettes (usually of 1- or 2-mm path length) can also be inserted in the place of this filter, and they can be filled with any solution of any concentration, thereby the properties of the filter can be tailored to the needs of the experimenter. For example, a cuvette filled with chloroform was used as a cut-off filter in one of our earlier works [10], whereas potassium nitrate solutions with different concentrations were used as filter to control the light intensity systematically in the same study [10] (Fig. 4).

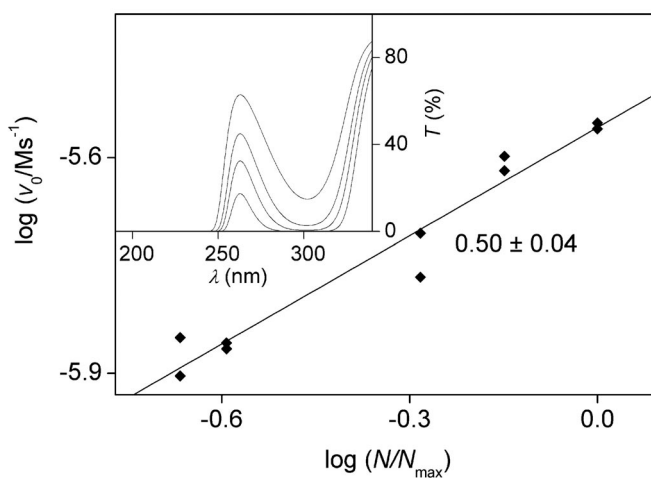


Fig. 4 Dependence of the reaction rate on the photon count in the photoinitiated and iodide-catalyzed autoxidation of S(IV) using intensity change by KNO_3 filter solutions. Inset: spectra of filter solutions (concentrations from highest to lowest transmissions: 0.5 M, 1.0 M, 1.5 M, 2.6 M). $[\text{I}^-] = 0.20\text{ mM}$, $[\text{S(IV)}] = 2.00\text{ mM}$, $[\text{H}_2\text{SO}_4] = 0.575\text{ M}$, path length: 1.000 cm, $T = 25.0\text{ }^{\circ}\text{C}$.

Some photochemical information can also be gained by systematically changing the illumination time patterns. The individual design of instruments must be carefully inspected before studies like these. For example, in a time-dependent mode, the Shimadzu instrument we used continuously irradiated the sample irrespective of the actual measurement periods. However, the HP instrument usually only illuminates the sample for measurement periods. This makes it possible to design experiments with interrupted illumination. The average rate of reaction from such experiments can reveal valuable information about the studied process. A simple photochemical reaction measured to low conversion should usually give an amount of product that is directly proportional to the illumination time. In the most advantageous evaluation, this translates into a direct proportionality between the average rate and the illumination ratio (which is the portion of time which the sample spends under illumination compared to the total time elapsed). An example of a simple photochemical reaction is shown in Fig. 5 where the autoxidation of S(IV) is monitored by using either continuous illumination or a sequence of 10 % illuminated and 90 % dark periods [8]. As expected, the rates of the two kinetic runs differ by a factor of 10. The lack of such proportionality is unambiguous proof of considerable progress of the studied reaction in the dark periods. A rigorous mathematical analysis of such effects can be used to reveal information about the termination step of photochemically initiated chain reactions [9].

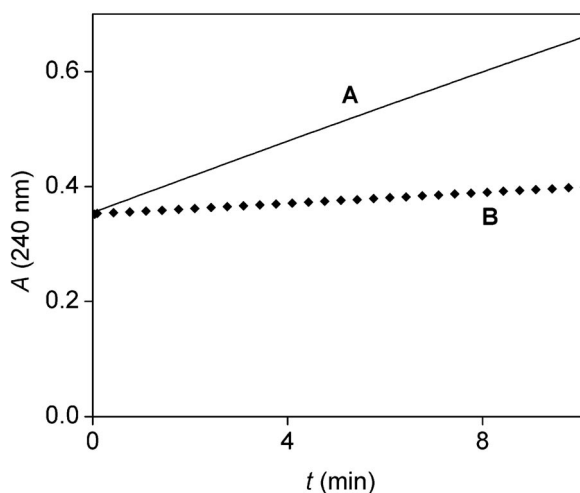


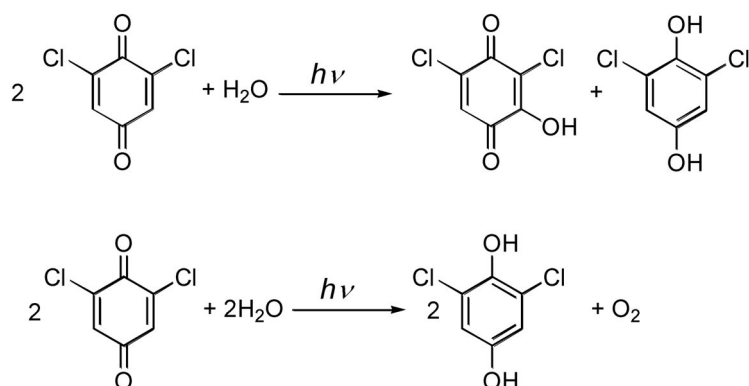
Fig. 5 Kinetic curves during the photochemical autoxidation of S(IV) in the presence of Fe(II): pH = 0.00, [S(IV)] = 2.00 mM, [Fe²⁺] = 5.20 mM, [O₂] = 0.23 mM, [HClO₄] = 1.0 M, path length: 1.000 cm, V = 2.00 cm³, illumination ratio: 100 % (A), 10 % (B).

LIGHT-INDUCED REDOX REACTIONS IN AQUEOUS SOLUTION

This section provides a few examples for the application of the principles and methods discussed above to explore specific details of complex redox reactions.

Aqueous photoreactions of 2,6-dichloro-1,4-benzoquinone (DCQ)

Quinones are often colored compounds and are active in various photochemical processes. The possibility of the systematic use of a diode-array spectrophotometer as a photochemical device was demonstrated on the aqueous photoreaction of DCQ [7], which is an important process in the destructive chemical oxidation of chlorophenols [14–16]. The photochemical reaction itself is known from the previously studied chemistry of other quinones [17–19]. It is a combination of two processes: the first is a water-assisted disproportionation of DCQ, the other is the photoreduction of DCQ by water (Scheme 2).



Scheme 2 Overall photochemical reactions in the aqueous solution of DCQ.

This system is a perfect candidate to demonstrate the general principles discussed in the previous paragraphs. First of all, the initial substance is yellow and the oxidation product 2,6-dichloro-3-hydroxy-1,4-benzoquinone is very intense purple. Therefore, the reaction could be monitored quite selectively with spectrophotometry. Second, the process has a high primary quantum yield close to 1, but is still a simple photochemical reaction. This is illustrated in Fig. 1 by the fact that the experimental kinetic curves are practically independent of temperature. Third, DCQ absorbs somewhat in the visible spectrum range as well. Therefore, as also shown in Fig. 1, a very spectacular demonstration of the photochemical nature of the studies process was possible: the reaction was much slower but did not stop when the experiment was repeated under identical conditions but with the UV lamp of the spectrophotometer turned off. Additional advantages included the fact that the spectrum of DCQ was quite fortunate in a sense that the amount of absorbed light could be changed significantly just by changing the reactant concentration (Fig. 2), and it was also possible to use an inner filter (NaNO_3) added to the reaction mixture to vary the photon count. Some isotope labeling was also convenient as demonstrated in Fig. 2. The reaction proceeded at basically the same rate in D_2O as in H_2O , but switching from DCQ to DCQ- d_2 (deuterating the reactant) revealed a kinetic isotope effect of 1.49. A study of the inhibitory effect of dimethyl sulfoxide was also conveniently carried out, and the use of eqs. 6–9 was demonstrated by simulating full kinetic traces by numerical integration [7]. Independent later studies with conventional photochemical methods verified many of the conclusions [20].

Autoxidation of S(IV)

The reaction of dissolved S(IV) with aerial oxygen is a thermodynamically favorable process



This reaction is the major source of acid rain formation, it is also a fundamental part of the desulfurization of flue gases and finds applications in epoxidation, food chemistry, metallurgical processes, etc. [21–25]. Environmental relevance and industrial application have driven considerable interest in the kinetics and mechanism of the overall process which exhibits complex behavior as a function of reactant concentrations and pH. Although various aspects of this reaction are still to be clarified, there seems to be consensus regarding some basic features. Under acidic conditions, the reaction is extremely slow and is believed to occur due to the presence of impurities acting as catalysts. The addition of various metal ions triggers a very efficient catalytic path of the oxidation. Fe(III) and Mn(II) are the most intensively studied catalysts in this system. There is ample evidence that the catalytic reactions progress through a radical-type chain mechanism which involves the formation of the $\text{SO}_3^{\cdot-}$ radical in

the initiation phase. Our kinetic studies on related systems indicated that the autoxidation is accelerated by Ce(III) and I^- under certain conditions [26]. Follow-up studies confirmed that these species act as catalyst only when the reaction mixture is illuminated [9,10].

The effect of light on the autoxidation of S(IV) is demonstrated in Fig. 6 [8–10]. The concentration of dissolved oxygen is monitored by using an oxygen meter in these systems. Oxygen consumption does not occur under normal laboratory light conditions in the absence of catalyst or when Fe(II) and Ce(III) are added as catalysts. Oxygen decay is triggered by turning on the illuminating light source in these systems. Slow oxidation of iodide ion under acidic conditions leads to oxygen consumption even in the absence of light. However, the reaction becomes considerably faster when the reaction mixture is illuminated, indicating again photochemical effects in this system. For technical reasons, these experiments were carried out in an open reactor, and diffusion of ambient oxygen into the reaction mixtures most likely biased the results. Accordingly, these experiments provide only semi-quantitative kinetic information on the reacting systems. Quantitative kinetic measurements were made in a diode-array spectrophotometer in sealed quartz cuvettes. In the absence of catalysts, the spectral change is consistent with the steady decay of S(IV) (Fig. 7). The same kind of experiments led to the decay of S(IV) and the formation of Fe(III) when the reaction mixture contained Fe(II). In the presence of Ce(III) and iodide ion, relatively fast decay of S(IV) was observed. The kinetic traces in these systems exhibit a characteristic brake point when the total amount of dissolved oxygen is consumed (Fig. 8). The analysis of the reaction mixtures confirmed that the only detectable sulfur product of the autoxidation is SO_4^{2-} in all of the studied systems.

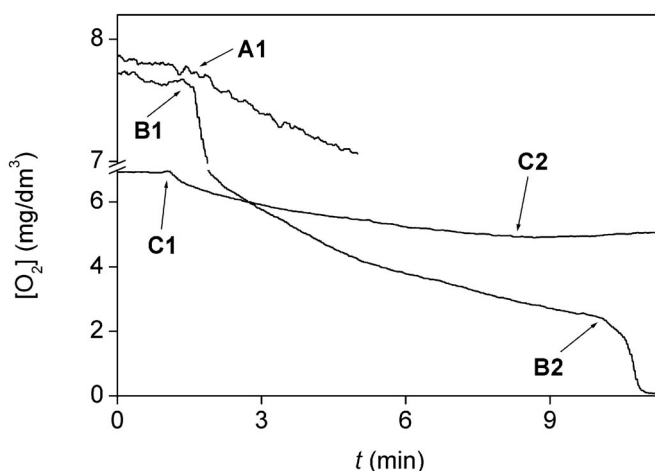


Fig. 6 Effect of light on the dissolved oxygen concentration in the photoinitiated autoxidation of S(IV) ($T = 25\text{ }^{\circ}\text{C}$ for all systems). (A) Reaction without catalyst, $[S(IV)] = 1.00\text{ mM}$; $[H_2SO_4] = 0.10\text{ M}$, **A1**: start of illumination. (B) Iodide ion catalysis $[I^-] = 0.20\text{ mM}$, $[S(IV)] = 2.0\text{ mM}$, $[HClO_4] = 0.10\text{ M}$, **B1**: addition of iodide ion to previously illuminated sample, **B2**: increase in illumination intensity by more than an order of magnitude (C) Ce(III) catalysis, $[Ce^{3+}] = 0.50\text{ mM}$; $[S(IV)] = 1.00\text{ mM}$; $[H_2SO_4] = 0.10\text{ M}$. **C1**: start of illumination, **C2**: end of illumination.

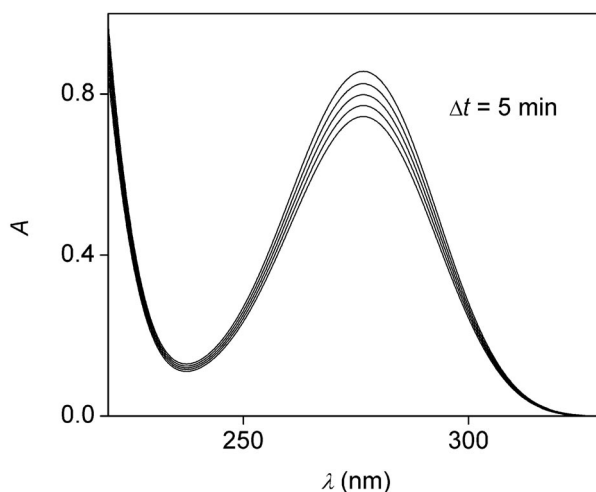


Fig. 7 Spectra measured in the uncatalyzed photochemical autoxidation of S(IV). [S(IV)] = 2.00 mM, [O₂] = 0.23 mM, [H₂SO₄] = 0.50 M, path length = 1.000 cm, $V = 2.00 \text{ cm}^3$; $T = 25.0 \text{ }^\circ\text{C}$. The absorbance band is characteristic for H₂O·SO₂ with $\lambda_{\text{max}} = 276 \text{ nm}$.

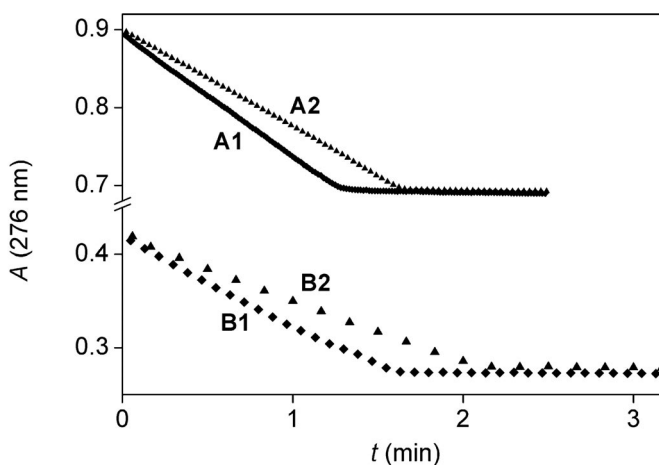


Fig. 8 Representative kinetic traces in the catalyzed, photoinitiated autoxidation of S(IV) ($V = 3.00 \text{ cm}^3$, $T = 25.0 \text{ }^\circ\text{C}$ and path length = 1.000 cm for all experiments). (A) Iodide ion catalysis. [I⁻] = 0.050 mM; [S(IV)] = 2.0 mM; [O₂] = 0.20 mM; [H₂SO₄] = 0.575 M, illumination ratio: 100 %, **A1**: direct light, **A2**: light with filter (B) Ce(III) catalysis [Ce³⁺] = 0.50 mM, [S(IV)] = 1.00 mM, [O₂] = 0.19 mM, [H₂SO₄] = 0.10 M, illumination ratio: 100 % (**B1**), 50 % (**B2**).

The kinetic traces are straight lines, although a slight deviation from this pattern was observed in the S(IV)–I⁻ system. This and the very small temperature dependence of the reaction rates are clear indications that the overall autoxidation reactions are photochemically controlled. The formation of Fe(III) as a by-product in the S(IV)–Fe(II) system is not unexpected because both of the reactants may act as a reducing agent toward dissolved oxygen. In this case, the progress of the reaction was also characterized by introducing the redox-equivalent product yield, $\omega = 2[\text{S(VI)}] + [\text{Fe(III)}]$ [8]. If the two products formed only via the oxidation of S(IV) and Fe(II) by the same oxidant, ω would be independent of the initial concentration of Fe(II) at any moment of the overall reaction, provided that the initial

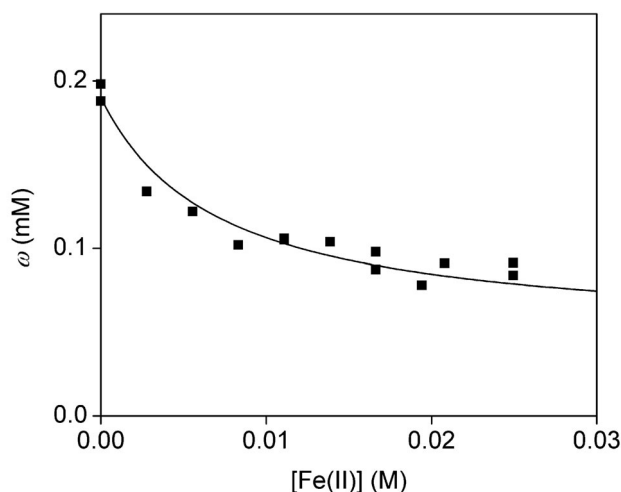


Fig. 9 The Fe(II) concentration dependence of the redox-equivalent product yield in the photochemically driven autoxidation of S(IV) in the presence of Fe(II): pH = 0.00, [S(IV)] = 2.00 mM; [O₂] = 0.23 mM; [HClO₄] = 1.0 M; reaction time: 900 s.

concentration of S(IV) is constant. However, the experimental results show a clear decay of ω as a function of [Fe(II)] (Fig. 9).

The rate of oxidation as a function of light intensity was studied in all of these systems using different experimental techniques. These experiments made it possible to determine the reaction orders with respect to the “light intensity” which is defined as photon count N . The concentration dependencies of the overall reaction rates were also studied in detail, and the reaction orders with respect to the reactants were determined. The results are summarized in Table 1. The kinetic models describing these reactions are presented in Tables 2–4, and their main features are discussed in the subsequent paragraphs together with some of the experimental results.

Table 1 Essential features of the photoinduced autoxidation of S(IV) in different systems.

		S(IV)	Fe(II)	Ce(III)	I ⁻
Order of reaction	Light	1	1	0.5	0.5
	O ₂	0	0	0	0
	S(IV)	0	0	0	Complicated rational function
	Catalyst	–	0	1	Complicated rational function
Absorbing species		S(IV)	S(IV)	Ce(III)	S(IV) and I ⁻
Temperature dependence		None	None	Slight	Slight
pH dependence in the studied region		None	None	None	Resembles the deprotonation of H ₂ O·SO ₂
Quantum yield for O ₂ loss		0.35	<0.35	50–500	100–1000
Remark		–	Energy transfer from S(IV)* to Fe(II)		Energy transfer from S(IV)* to I ⁻

Table 2 Individual reaction steps in the autoxidation of S(IV) in the presence of Fe(II).

Reaction	Type ^a
$\text{H}_2\text{O}\cdot\text{SO}_2 \rightleftharpoons \text{HSO}_3 + \text{H}^+$	E
$\text{H}_2\text{O}\cdot\text{SO}_2 + h\nu \rightarrow \text{*H}_2\text{O}\cdot\text{SO}_2$	P
$\text{*H}_2\text{O}\cdot\text{SO}_2 + \text{O}_2 \rightarrow \text{HSO}_5^- + \text{H}^+$	L
$\text{*H}_2\text{O}\cdot\text{SO}_2 + \text{Fe(II)} \rightarrow \text{H}_2\text{O}\cdot\text{SO}_2 + \text{*Fe(II)}$	L
$\text{*Fe(II)} + \text{H}^+ \rightarrow \text{Fe(III)} + \frac{1}{2}\text{H}_2$	S
$\text{HSO}_5^- + \text{H}_2\text{O}\cdot\text{SO}_2 \rightarrow 2\text{HSO}_4^- + \text{H}^+$	L
$\text{HSO}_5^- + 2\text{Fe}^{2+} \rightarrow 2\text{Fe}^{3+} + \text{HSO}_4^-$	S

^aE: fast equilibrium; P: primary photochemical process; L: thermal elementary step; S: fast series of elementary steps.

Table 3 Individual reaction steps in the Ce(III)-catalyzed autoxidation of S(IV).

Reaction	Type ^a
$\text{H}_2\text{O}\cdot\text{SO}_2 \rightleftharpoons \text{HSO}_3 + \text{H}^+$	E
$\text{Ce}^{3+} + \text{H}^+ + h\nu \rightarrow \text{Ce}^{4+} + 0.5\text{H}_2$	P
$\text{Ce}^{4+} + \text{H}_2\text{O}\cdot\text{SO}_2 \rightarrow \text{SO}_3^{\cdot-} + \text{Ce}^{3+} + 2\text{H}^+$	L
$\text{SO}_3^{\cdot-} + \text{O}_2 \rightarrow \text{SO}_5^{\cdot-}$	L
$\text{SO}_5^{\cdot-} + \text{H}_2\text{O}\cdot\text{SO}_2 \rightarrow \text{SO}_4^{\cdot-} + \text{HSO}_4^- + \text{H}^+$	L
$\text{SO}_4^{\cdot-} + \text{Ce}^{3+} + \text{H}^+ \rightarrow \text{Ce}^{4+} + \text{HSO}_4^-$	L
$\text{SO}_4^{\cdot-} + \text{SO}_4^{\cdot-} \rightarrow \text{S}_2\text{O}_8^{2-}$	L

^aE: fast equilibrium; P: primary photochemical process; L: thermal elementary step.

Table 4 Individual reaction steps in the iodide ion-catalyzed autoxidation of S(IV).

Reaction	Type ^a
$\text{H}_2\text{O}\cdot\text{SO}_2 \rightleftharpoons \text{HSO}_3 + \text{H}^+$	E
$\text{H}_2\text{O}\cdot\text{SO}_2 + h\nu \rightarrow \text{*H}_2\text{O}\cdot\text{SO}_2$	P
$\text{I}^- + h\nu + \text{H}_2\text{O}\cdot\text{SO}_2 + \text{O}_2 \rightarrow \text{I}^{\cdot} + \text{SO}_4^{\cdot-} + \text{H}_2\text{O}$	P
$\text{*H}_2\text{O}\cdot\text{SO}_2 + \text{I}^- + \text{O}_2 \rightarrow \text{I}^{\cdot} + \text{SO}_4^{\cdot-} + \text{H}_2\text{O}$	S
$\text{SO}_3^{\cdot-} + \text{O}_2 \rightarrow \text{SO}_5^{\cdot-}$	L
$\text{SO}_5^{\cdot-} + \text{H}_2\text{O}\cdot\text{SO}_2 \rightarrow \text{SO}_4^{\cdot-} + \text{HSO}_4^- + \text{H}^+$	L
$\text{SO}_4^{\cdot-} + \text{SO}_4^{\cdot-} \rightarrow \text{S}_2\text{O}_8^{2-}$	L
$\text{SO}_4^{\cdot-} + \text{I}^- \rightarrow \text{I}^{\cdot} + \text{SO}_4^{2-}$	L
$\text{I}^{\cdot} + \text{H}_2\text{O}\cdot\text{SO}_2 \rightarrow \text{SO}_3^{\cdot-} + \text{I}^- + 2\text{H}^+$	L
$\text{I}^{\cdot} + \text{HSO}_3^- \rightarrow \text{SO}_3^{\cdot-} + \text{I}^- + \text{H}^+$	L
$\text{I}^- + \text{I}^{\cdot} = \text{I}_2^{\cdot-}$	R
$\text{I}_2^{\cdot-} + \text{H}_2\text{O}\cdot\text{SO}_2 \rightarrow \text{SO}_3^{\cdot-} + 2\text{I}^- + 2\text{H}^+$	L
$\text{I}_2^{\cdot-} + \text{HSO}_3^- \rightarrow \text{SO}_3^{\cdot-} + 2\text{I}^- + \text{H}^+$	L
$\text{I}_2^{\cdot-} + \text{I}_2^{\cdot-} \rightarrow \text{I}^- + \text{I}_3^-$	L
$\text{SO}_4^{\cdot-} + \text{I}_2^{\cdot-} \rightarrow \text{SO}_4^{2-} + \text{I}_2$	L
$\text{I}_2 + \text{I}^- = \text{I}_3^-$	E
$\text{I}_2 + \text{H}_2\text{O}\cdot\text{SO}_2 + \text{H}_2\text{O} \rightarrow \text{HSO}_4^- + 2\text{I}^- + 3\text{H}^+$	S

^aE: fast equilibrium; P: primary photochemical process; L: thermal elementary step; S: fast series of elementary steps; R: reversible elementary steps.

The observations in the S(IV)–Fe(II) system confirmed that the overall process is purely photochemical. However, this kinetic pattern changes considerably when the pH is increased due to the fact that thermally activated catalytic autoxidation of S(IV) sets on. The S(IV)–Ce(III) system exhibits very different kinetic features (Fig. 10). In this case, the reaction rate is clearly dependent on the duration of the dark period even when the amount of the illuminating light does not change, i.e., the illumination ratio is constant. This indicates that a significant portion of the overall process takes place in the dark period. It was concluded that the reaction rate is constant during the illumination period (cf. the linearity of the kinetic traces) but decays sharply in the dark phase. It can be shown that the average reaction rate is higher when the dark periods are shorter even if the same amount of light enters the sample [9].

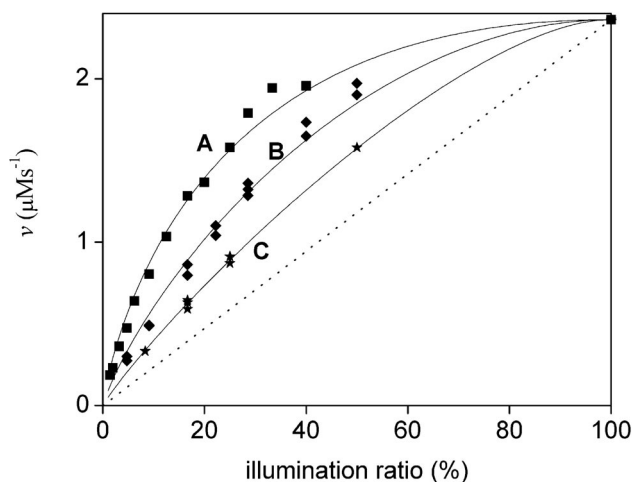


Fig. 10 Average reaction rate as a function of the illumination ratio in the Ce(III)-catalyzed autoxidation of S(IV). $[Ce^{3+}] = 0.50 \text{ mM}$; $[S(IV)] = 1.00 \text{ mM}$; $[H_2SO_4] = 0.10 \text{ M}$; $V = 3.00 \text{ cm}^3$; $T = 25.0 \text{ }^\circ\text{C}$; illumination times: 1 s (A), 2 s (B), 5 s (C).

An inspection of Table 1 reveals that the general photochemical features of the overall reactions are very similar in the presence of Ce(III) and I^- , i.e., the reaction rates are about half order in light intensity and the quantum yields are very high. The above conclusions regarding the intermittent dark periods and the results in Table 1 are consistent with a radical-type chain reaction mechanism in both systems. It is assumed that the primary photochemical reactions lead to the formation of reactive radicals, which trigger very efficient propagation steps. The chain is maintained by fast regeneration of the $SO_3^{\cdot-}$ radical in both systems. Termination of the chain occurs in a slow step via the recombination of the $SO_4^{\cdot-}$ radical, thus, the concentration of $S_2O_8^{2-}$ formed in this step is negligible to that of SO_4^{2-} , which is formed mainly in the propagation steps.

In the absence of catalyst, the autoxidation of S(IV) proceeds via the formation of HSO_5^- . It is well known that the oxidation by O_2 is spin-forbidden in most cases. The generation of the excited $H_2O \cdot SO_2$ species opens a favorable reaction path for the activation of O_2 . When Fe(II) is present, an alternative reaction path of the oxidation needs to be considered. The decay of the equivalent product yield (Fig. 7) can be interpreted in terms of sensitizing of Fe(II). This reaction sequence opens a new reaction channel for the removal of excited S(IV) and leads to the formation of half as much Fe(III) than the reaction via HSO_5^- .

Energy transfer also needs to be assumed for the interpretation of the results in the presence of iodide ion. When experiments were carried out by excluding most of the light absorption by I^- the dominant absorbing species was $H_2O \cdot SO_2$. Still, the photochemically induced autoxidation was orders of

magnitude faster than in the absence of I^- . This observation implies that the excited S(IV) species opens an efficient initiation sequence which includes I^- .

As demonstrated in Figs. 9–11, the proposed kinetic models provide an excellent interpretation of the experimental observations in the photoinitiated autoxidation of S(IV) in the absence and the presence of catalysts.

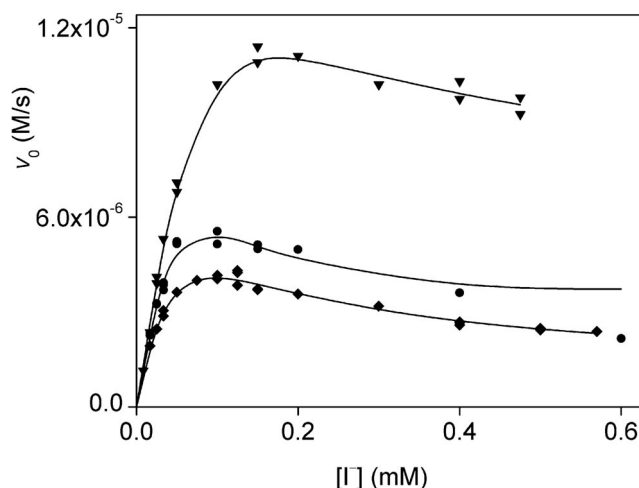


Fig. 11 Dependence of the initial rate on the concentration of iodide ion in the photoinitiated and iodide-catalyzed autoxidation of S(IV). [S(IV)] = 2.00 mM (triangles), 1.00 mM (circles), 0.70 mM (diamonds), [H₂SO₄] = 0.575 M, V = 3.00 cm³, T = 25.0 °C.

A photochemically activated redox reaction of the chlorate ion

Chlorate ion is a potent but kinetically inert oxidant in aqueous solution ($\epsilon_0 = 1.16$ V, for Cl(V)/Cl(III) in 1.0 M [H⁺] [27]) and it does not oxidize even strong reducing agents. Thus, chlorate ion is often postulated as a final product in the reactions of oxychlorine species. Due to the noted inertness, chlorate ion does not oxidize iodine under acidic conditions and in the absence of light even though the reaction would thermodynamically be favored. However, when a solution containing ClO₃⁻ and I₂ is illuminated in a diode-array spectrophotometer, the disappearance of iodine is observed after a certain incubation period (Fig. 12) [4,5]. It was confirmed that the overall reaction proceeds according to the following stoichiometry:



The reaction shows autocatalytic features. It was established that the duration of the incubation period depends on the total amount of light passing the sample, but the subsequent kinetic process is independent of light intensity [5]. It could easily be confirmed that the photoactive species is I₂ in this system. The observations were interpreted by assuming that an autocatalytic species is accumulated photochemically in the first phase of the reaction. Once the concentration of the autocatalytic species reaches a sufficiently high level, the thermally activated reaction steps become dominant. This is proved by the inset of Fig. 12, where the kinetic trace measured with the UV light switched on matches the curves measured under identical conditions but only with visible illuminations, however, the incubation period is longer in the second case. The addition of minute amounts of HOCl or ClO₂⁻ to a reaction mixture triggered the immediate decay of I₂ in the absence of light, confirming that these species are probably the autocatalysts formed in the incubation periods [5]. The kinetic model postulated for this

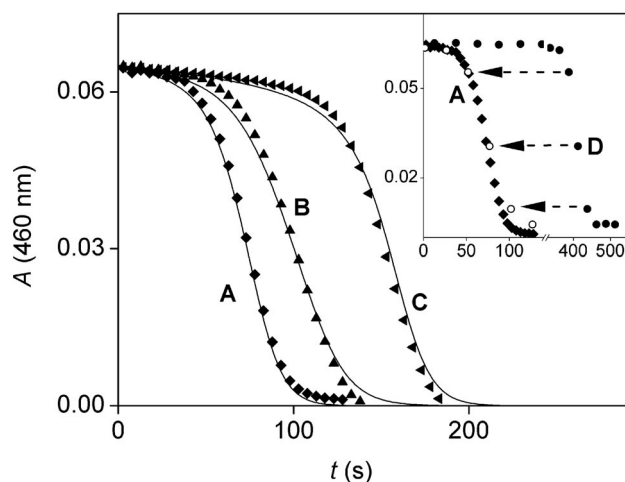


Fig. 12 Measured (markers) and fitted (lines) kinetic curves in the photoinitiated oxidation of I_2 by ClO_3^- . Inset: comparison of experiments with a difference in lamp use. $[I_2] = 88 \mu\text{M}$; $[ClO_3^-] = 25.1 \text{ mM}$ (A, C, D), 16.7 mM (B), $[H^+] = 0.948 \text{ M}$ (A, B, D), 0.356 M (C); continuous illumination (A, B, C), continuous illumination with visible lamp only (D), $T = 25.0 \text{ }^\circ\text{C}$.

system is shown in Table 5. It is assumed that the first step of the reaction is photochemical dissociation of iodine into I^\bullet radicals, which react quickly with ClO_3^- to form the $IClO_3^{\bullet-}$ radical. This species decomposes in a subsequent reaction and forms a series of reactive intermediates which are converted into the final products in further reaction steps. Figure 12 demonstrates the fit of the model to the experimental data.

Table 5 Individual reaction steps in the iodide ion catalyzed autoxidation of S(IV).

Reaction	Type ^a
$I_2 + ClO_3^- + H_2O + h\nu \rightarrow IO_3^- + H_2OI^+ + Cl^-$	P
$HOCl + H^+ + Cl^- \rightleftharpoons Cl_2 + H_2O$	E
$H_2OI^+ + ClO_3^- \rightarrow IO_3^- + HOCl + H^+$	S*
$H_2OI^+ + 2HOCl \rightarrow IO_3^- + 2Cl^- + 4H^+$	S*
$I_2 + Cl_2 + 2H_2O \rightarrow 2H_2OI^+ + 2Cl^-$	S*

^aE: fast equilibrium; P: primary photochemical process; S*: series of elementary steps with the first being rate-determining.

SUMMARY

The previous examples clearly demonstrate that photochemical studies in commercially available diode-array spectrophotometers can conveniently be used to obtain crucial kinetic and mechanistic information on a variety of photoinduced chemical reactions. Our recent results [28] and preliminary studies on further redox reactions indicate that photochemistry may interfere with thermally activated reactions during spectrophotometric measurements more often than anticipated in the relevant literature. This also justifies a strong warning that failure to test for the possible photochemical role of the intense light of a diode-array spectrophotometer may lead to biased experimental results and erroneous conclusions.

Some of our published results [7] have already been confirmed by more conventional photochemical methods [20], which indicates the reliability of using spectrophotometers for such studies. We feel that the advantage of our approach is the simple instrumentation needed and the fact that the driving light imitates the spectral distribution of sunlight, the use of which is a primary goal of practical photochemistry.

ACKNOWLEDGMENT

The Hungarian Research Fund is acknowledged for financial support under Grant Nos. OTKA K68668 and F049498.

REFERENCES

1. J. W. Robinson. *Undergraduate Instrumental Analysis*, 5th ed., pp. 258–314, Marcel Dekker, New York (1995).
2. H. W. Willard, L. L. Merritt, J. A. Dean, F. A. Settle Jr. *Instrumental Methods of Analysis*, 7th ed., pp. 159–196, Wadsworth, Belmont, CA (1988).
3. M. Thomas. *Ultraviolet and Visible Spectroscopy: Analytical Chemistry by Open Learning*, 2nd ed., John Wiley, London (1996).
4. A. P. Oliveira, R. B. Faria. *J. Am. Chem. Soc.* **127**, 18022 (2005).
5. M. Galajda, G. Lente, I. Fábián. *J. Am. Chem. Soc.* **129**, 7738 (2007).
6. D. M. Stanbury, J. N. Figlar. *Coord. Chem. Rev.* **187**, 223 (1999).
7. G. Lente, J. H. Espenson. *J. Photochem. Photobiol. A* **163**, 249 (2004).
8. I. Kerezsi, G. Lente, I. Fábián. *Dalton Trans.* 955 (2006).
9. I. Kerezsi, G. Lente, I. Fábián. *J. Am. Chem. Soc.* **127**, 4785 (2005).
10. I. Kerezsi, G. Lente, I. Fábián. *Inorg. Chem.* **46**, 4230 (2007).
11. J. W. Verhoeven. *Pure Appl. Chem.* **68**, 2223 (1996).
12. C. G. Hatchard, C. A. Parker. *Proc. R. Soc. London, Ser. A* **235**, 518 (1956).
13. N. J. Bunce. In *CRC Handbook of Organic Photochemistry*, Vol. 1, J. C. Scaiano (Ed.), pp. 241–259, CRC Press, Boca Raton (1989).
14. G. Lente, J. H. Espenson. *Chem. Commun.* 1162 (2003).
15. G. Lente, J. H. Espenson. *Int. J. Chem. Kinet.* **36**, 449 (2004).
16. G. Lente, J. H. Espenson. *New J. Chem.* **28**, 847 (2004).
17. J. M. Bruce, E. Cutts. *J. Chem. Soc. C* 449 (1966).
18. A. E. Alegría, A. Ferrer, E. Sepúlveda. *Photochem. Photobiol.* **66**, 436 (1997).
19. A. E. Alegría, A. Ferrer, G. Santiago, E. Sepúlveda, W. Flores. *J. Photochem. Photobiol. A* **127**, 57 (1999).
20. H. Görner, C. von Sonntag. *J. Phys. Chem. A* **112**, 10257 (2008).
21. E. H. Cho. *Metall. Trans. B* **17**, 745 (1986).
22. C. Brandt, I. Fábián, R. van Eldik. *Inorg. Chem.* **33**, 687 (1994).
23. C. Brandt, R. van Eldik. *Chem. Rev.* **95**, 119 (1995).
24. V. Csordás, I. Fábián. *Adv. Inorg. Chem.* **54**, 395 (2003).
25. R. F. McFeeters, L. M. Barrangou, A. O. Barish, S. S. Morrison. *J. Agric. Food Chem.* **52**, 4554 (2004).
26. G. Lente, I. Fábián. *Inorg. Chem.* **43**, 4019 (2004).
27. S. G. Bratsch. *J. Phys. Chem. Ref. Data* **18**, 1 (1989).
28. G. Lente, J. Kalmár, Z. Baranyai, A. Kun, I. Kék, D. Bajusz, M. Takács, L. Veres, I. Fábián. *Inorg. Chem.* **48**, 1763 (2009).